NONLINEAR OPTICAL PHENOMENA

PACS numbers: 42.40.Eq; 42.70.Nq
DOI: 10.1070/QE2001v031n11ABEH002086

Nonunidirectional energy exchange upon the steady-state two-wave interaction in a cubic gyrotropic photorefractive crystal in a dc electric field

R V Litvinov, S M Shandarov

Abstract. **The steady-state two-wave interaction on a transmission photorefractive grating produced in a cubic gyrotropic crystal of the symmetry group 23 in an external dc electric field is studied. The analytic solution of the equation for coupled waves is obtained for an arbitrary orientation of the crystal and arbitrary polarisation of incident light beams in the fixed pump approximation. It is shown that a nonunidirectional contribution to the energy exchange between the waves can exist, which is caused by the local component of the photorefractive grating. In a particular case of light waves with a wavelength of 633 nm propagating in the (001) plane of a $Bi_{12}TiO_{20}$ crystal and of the orientation of the grating vector along the [$\bar{1}$10] axis, this contribution greatly exceeds a usual unidirectional contribution. The dependence of the two-wave gain on the modulation coefficient of the interference pattern on the input face of the crystal is studied by numerically integrating a total system of coupled-wave equations.**

Keywords: *photorefractive grating, two-wave interaction, gyrotropic crystal.*

1. Introduction

The interaction of two light waves on dynamic phase holograms formed by them in a photorefractive crystal has been studied over more than 30 years [1 – 9]. The results of these studies are used for amplification of weak light signals, data recording, storage, and reading [8, 9]. Current interest in the two-wave interaction [10 – 17] is caused by the fact that complicated multiwave interactions that are used in applications of modern photorefractive optics [8, 9, 18, 19] represent a set of coupled two-wave processes.

A permittivity grating produced upon the interaction of two plane light waves in a photorefractive crystal is shifted in the general case with respect to the interference pattern. This shift depends on the mechanism of transfer of charge carriers excited by light, which induces an electric field in the crystal [8, 9, 18]. Upon the stationary two-wave interaction on a photorefractive grating of the diffusion type, such a shift is equal to a quarter of the spatial period ($\Lambda/4$). Analysis of coupled-wave equations neglecting the transformation of the polarisation structure of a light field during the interaction shows that such a nonlocal photorefractive response results in the redistribution of energy between the interacting waves, their phases being unchanged.

A photorefractive grating produced due to the nonlinear photogalvanic effect is shifted with respect to the interference pattern by $\Lambda/2$. Such a local response changes the phases of the interacting waves but does not change their intensity [3 – 5, 7 – 9, 18]. The energy transfer between the light waves on the local grating can occur upon the nonstationary interaction, for example, upon writing or reading of a photorefractive hologram [4, 6]. It follows from the scalar theory of the steady-state interaction of two plane light waves in the case of nonlocal photorefractive response of a medium that, by neglecting the photogalvanic effect and the absorption grating, the direction of energy transfer from one wave to another depends only on the orientation of the vector $\boldsymbol{K}$ of the photorefractive grating with respect to the crystallophysic coordinate system, while a change in the ratio of intensities of the beams does not affect the direction of energy transfer [3 – 5, 7 – 9].

The studies of nonstationary mechanisms of the formation of photorefractive holograms in cubic photorefractive crystals $Bi_{12}GeO_{20}$, $Bi_{12}SiO_{20}$, $Bi_{12}TiO_{20}$, GaAs, etc. in the presence of a static light-intensity grating in an external ac electric field or of a grating travelling in a dc electric field [8, 9] showed a strong influence of the vector nature of the two-wave interaction on the energy-transfer efficiency [10 – 17]. The coupled-wave equations were recently analysed, taking into account the transformation of the polarisation structure of the light field caused by the interaction in the presence of the natural circular and external field-induced linear birefringence, in papers [10, 13, 17]. It was shown that the energy exchange between the light waves interacting on the nonlocal photorefractive grating also contains a nonunidirectional component, which always amplifies a weak wave. This result was experimentally confirmed in paper [14].

In this paper, we consider the steady-state energy exchange upon the interaction of two plane monochromatic light waves on a transmission photorefractive grating containing the local and nonlocal components, which was produced in a cubic gyrotropic crystal of the symmetry group 23 in an external dc electric field, taking into account the transformation of the polarisation structure of the light field caused by the interaction of the waves. For simplicity,

R V Litvinov, S M Shandarov Division of Electronic Devices, Tomsk State University of Control Systems and Radioelectronics, prosp. Lenina 40, 634050 Tomsk, Russia;
e-mail: shand@stack.ru

Received 12 April 2001
Kvantovaya Elektronika **31** (11) 973 – 980 (2001)
Translated by M N Sapozhnikov

we neglected absorption of light and additional contributions from the photoelastic and piezoelectric effects to the modulation of the optical properties of the medium.

2. Theoretical model

The vector diagram of the symmetric two-wave interaction is shown in Fig. 1 for the case when an external electric field $\boldsymbol{E}_0$ is applied along the grating vector. Due to the natural circular and induced linear birefringence, the light field in a crystal can be represented as a superposition of four plane waves, which, in the paraxial approximation, have the form

$$\tilde{\boldsymbol{S}}_{1,2} = S_{1,2}(x)\boldsymbol{e}_{1,2}\exp\bigl[\mathrm{i}\bigl(\omega t - n_{1,2}kx + Kz/2\bigr)\bigr],$$
$$\tilde{\boldsymbol{R}}_{1,2} = R_{1,2}(x)\boldsymbol{e}_{1,2}\exp\bigl[\mathrm{i}\bigl(\omega t - n_{1,2}kx - Kz/2\bigr)\bigr], \quad (1)$$

where $n_{1,2}$ and $\boldsymbol{e}_{1,2}$ are the refractive indices and the normalised polarisation vectors of the natural waves of the medium, respectively, which correspond to the direction of propagation along the normal (the x axis) to the crystal boundary; $k = 2\pi/\lambda$ is the wave number of light in vacuum; and $K = 2\pi/\Lambda$. The amplitudes of the natural waves $S_j(x)$ and $R_j(x)$ are assumed dependent on x because of their interaction. The analytic expressions for the wave parameters $n_{1,2}$ and $\boldsymbol{e}_{1,2}$ are presented in papers [10, 20] for arbitrary orientations of an external field and the normal to the crystal face directed perpendicular to the field. For two particular cases of the interaction considered below, when the vector $\boldsymbol{K}$ of the photorefractive grating is oriented along the [001] axis and the light waves propagate in the $(\bar{1}10)$ plane (the longitudinal geometry) or when the vector $\boldsymbol{K}$ is parallel to the $[\bar{1}10]$ axis and the waves propagate in the (001) plane (the transverse geometry), the parameters $n_{1,2}$ and $\boldsymbol{e}_{1,2}$ can be obtained using expressions presented in Table 1.

Note that in the absence of an external electric field ($E_0 = 0$), the natural waves are circularly polarised with opposite directions of rotation, and the wave surfaces corresponding to the natural waves represent spheres with radii $nk \pm \rho$.

The perturbations of the permittivity induced by an external electric field ($E_0 \neq 0$) due to a linear electrooptical effect changes polarisation of the natural waves from circular to elliptical, retaining the initial direction of rotation. In the case of a longitudinal geometry, the polarisation ellipses are elongated along coordinate axes $y \,||\, [\bar{1}10]$ and $z \,||\, [001]$, respectively. In the case of a transverse geometry, these ellipses are elongated along the straight lines directed at angles $+45^\circ$ and -45° to the axis $z \,||\, [\bar{1}10]$. The wave surfaces are transformed to ellipsoids, which, unlike the wave surfaces of nongyrotropic media [21], have no common points. In the case of a longitudinal geometry, the sections of these surfaces by the plane of incidence $(\bar{1}10)$ of light waves give ellipses elongated along the direction of the applied electric field, the [001] axis. In the case of a transverse geometry, the similar sections by the (001) plane give ellipses elongated along the normal $\boldsymbol{x}_0 \,||\, [110]$ to the crystal boundary.

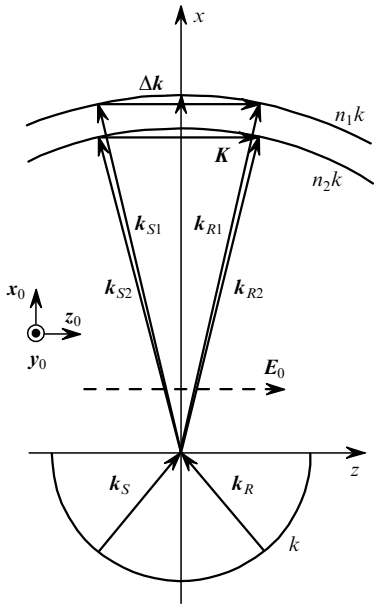

Figure 1. Vector diagram of the two-weave interaction on the transmission photorefractive grating in a cubic gyrotropic crystal in an external dc electric field ($\boldsymbol{k}_S$ and $\boldsymbol{k}_R$ are the wave vectors of the incident waves; $|\boldsymbol{k}_{R1,R2}| = |\boldsymbol{k}_{S1,S2}| = n_{1,2}k$).

In the steady-state two-wave interaction regime, the amplitude of the field of a spatial charge in the linear approximation over the modulation coefficient $m(x)$ of the interference pattern produced by plane monochromatic light waves (1) can be written in the form [8, 9]

$$E_1(x) = -m(x)\bigl(E' + \mathrm{i}E''\bigr), \quad (2)$$

where

$$m(x) = 2\frac{S_1(x)R_1^*(x) + S_2(x)R_2^*(x)}{I_0}; \quad (3)$$

$$E' = \frac{E_0E_\mathrm{q}^2}{(E_\mathrm{q}+E_\mathrm{d})^2+E_0^2}; \quad E'' = E_\mathrm{q}\frac{E_\mathrm{d}(E_\mathrm{q}+E_\mathrm{d})+E_0^2}{(E_\mathrm{q}+E_\mathrm{d})^2+E_0^2}; \quad (4)$$

Table 1. Refractive indices and polarisation vectors of natural waves, as well as tensor convolutions that determine the relation between the light waves of the same (g_{11} and g_{22}) and different (g_{12} and $g_{21} = g_{12}^*$) types for two particular orientations of the two-wave interaction in a cubic gyrotropic photorefractive crystal of the symmetry 23.

Geometry	Refractive indices	Polarisation vectors	Tensor convolutions
Longitudinal: $x \,||\, [110],\ z \,||\, [001]$	$n_{1,2} = n + (\delta n/2) \pm \Delta n$	$\boldsymbol{e}_1 = (\boldsymbol{y}_0 + \mathrm{i}r\boldsymbol{z}_0)/(1+r^2)^{1/2}$ $\boldsymbol{e}_2 = (r\boldsymbol{y}_0 - \mathrm{i}\boldsymbol{z}_0)/(1+r^2)^{1/2}$	$g_{11} = (\rho/k)^2/(\delta n\Delta n - 2\Delta n^2)$, $g_{22} = -1 - g_{11},\ g_{12} = -\rho/(2\Delta nk)$
Transverse: $x \,||\, [110],\ z \,||\, [\bar{1}10]$	$n_{1,2} = n \pm [(\rho/k)^2 + \delta n^2]^{1/2}$	$\boldsymbol{e}_1 = [\exp(-\mathrm{i}\varphi)\boldsymbol{y}_0 + \mathrm{i}\boldsymbol{z}_0]/\sqrt{2}$ $\boldsymbol{e}_2 = [\boldsymbol{y}_0 - \mathrm{i}\exp(\mathrm{i}\varphi)\boldsymbol{z}_0]/\sqrt{2}$	$g_{11} = -\delta n/[(\rho/k)^2 + \delta n^2]^{1/2}$, $g_{22} = -g_{11},\ g_{12} = 1/[(\delta nk/\rho) + \mathrm{i}]$

Notes: $\Delta n = [(\rho/k)^2 + (\delta n/2)^2]^{1/2}$; $r = (k/\rho)[\Delta n - (\delta n/2)]$; $\varphi = \arctan(\delta nk/\rho)$; $\delta n = n^3 r_{41}E_0/2$; n is the refractive index of the unperturbed crystal; r_{41} is the electrooptical coefficient; ρ is the specific optical rotation; $\boldsymbol{y}_0$ and $\boldsymbol{z}_0$ are the unit vectors of the coordinate system.

$$I_0 = \sum_{j=1}^{2} \left|S_j(x)\right|^2 + \left|R_j(x)\right|^2$$

is the average light intensity normalised to the coefficient $n/240\pi$, whose dimensionality is 1 Cm; E_0 is the applied electric field strength ($\boldsymbol{E}_0 = E_0 \boldsymbol{z}_0$); $E_d = 2\pi k_B T/\Lambda e$ is the diffusion field; $E_q = eN_a\Lambda/2\pi\varepsilon$ is the trap-saturation field; N_a is the acceptor concentration in the crystal; T is the absolute temperature; e is the elementary electric charge; and ε is the static permittivity of the crystal.

The coupled-wave equations can be obtained from the wave equation for gyrotropic media by the method of slowly varying amplitudes. Taking into account the known expressions for perturbations of the optical properties of the crystal caused by the linear electrooptical effect, we find

$$\frac{dS_1(x)}{dx} = \frac{\pi n^3 r_{41}\left(E'' - iE'\right)}{2\lambda} m(x) \times \left[g_{11}R_1(x) + g_{12}\exp(i\Delta kx)R_2(x)\right], \quad (5)$$

$$\frac{dS_2(x)}{dx} = \frac{\pi n^3 r_{41}\left(E'' - iE'\right)}{2\lambda} m(x) \times \left[g_{12}^* \exp(-i\Delta kx)R_1(x) + g_{22}R_2(x)\right], \quad (6)$$

$$\frac{dR_1(x)}{dx} = -\frac{\pi n^3 r_{41}\left(E'' + iE'\right)}{2\lambda} m^*(x) \times \left[g_{11}S_1(x) + g_{12}\exp(i\Delta kx)S_2(x)\right], \quad (7)$$

$$\frac{dR_2(x)}{dx} = -\frac{\pi n^3 r_{41}\left(E'' + iE'\right)}{2\lambda} m^*(x) \times \left[g_{12}^* \exp(-i\Delta kx)S_1(x) + g_{22}S_2(x)\right], \quad (8)$$

where $\Delta k = (n_1 - n_2)k$. For arbitrary orientations of the crystal and the grating vector, the tensor convolutions describing contributions of the intramode (g_{11}, g_{22}) and intermode (g_{12}) processes can be calculated using the relations presented in papers [10, 20]. For particular cases of the longitudinal and transverse geometry, these convolutions are presented in Table 1.

Coupled-wave equations (5)–(8) have the integral

$$|S_1|^2 + |S_2|^2 + |R_1|^2 + |R_2|^2 = I_0, \quad (9)$$

which corresponds to the fundamental law of conservation of the light-field energy during its redistribution between interacting beams in a nonabsorbing medium.

3. Interaction in the fixed pump wave approximation

The interaction under study can be analysed at small modulation coefficients $m(x) \ll 1$ of the interference pattern using the fixed pump-wave field approximation and assuming that the scalar amplitudes $R_j(x)$ are independent of x [$R_1(x) = R_1(0) \equiv R_{10}$ and $R_2(x) = R_2(0) \equiv R_{20}$]. In this case, we can obtain from equations (5) and (6) the expression for the modulation coefficient

$$m(x) = m_0 \exp\left[\frac{\pi n^3 r_{eff}(x)\left(E'' - iE'\right)x}{\lambda}\right], \quad (10)$$

where m_0 is the modulation coefficient for $x = 0$;

$$r_{eff}(x) = r_{41}\left\{\eta_{in} - 2\mathrm{Im}\left[\eta_{inter}\frac{1 - \exp(i\Delta kx)}{\Delta kx}\right]\right\} \quad (11)$$

is the effective electrooptical coefficient. The parameters $\eta_{in} = \left(g_{11}|R_{10}|^2 + g_{22}|R_{20}|^2\right)/I_0$ and $\eta_{inter} = g_{12}R_{10}^*R_{20}/I_0$ describe the contributions from intramode and intermode processes to the interaction, respectively, and determine the spatial dependences of the modulation coefficient and the field amplitude of the spatial charge [see expression (2)]. Note that the photorefractive grating with the amplitude proportional to $E_1(x)$ is shifted with respect to the interference pattern with the modulation coefficient $m(x)$ and contains the local and nonlocal components whose amplitudes are proportional to E' and E''.

The integration of equations (5) and (6), taking into account relations (10) and (11), gives the vector amplitude $\boldsymbol{S}(x) = S_1(x)\boldsymbol{e}_1 + S_2(x)\boldsymbol{e}_2\exp(i\Delta kx)$ of the total light field of the signal wave in the form

$$\boldsymbol{S}(x) = \boldsymbol{S}_{||}(x) + \frac{m_0}{2}\left\{\left[\exp\left(\frac{\pi n^3 r_{eff}(x)\left(E'' - iE'\right)x}{\lambda}\right) - 1\right]\boldsymbol{R}_{||}(x) + \frac{\pi n^3 r_{41}\left(E'' - iE'\right)}{\lambda}X(x)\boldsymbol{R}_{\perp}(x)\right\}, \quad (12)$$

where

$$X(x) = \int_0^x g(\zeta)\exp\left[\frac{\pi n^3 r_{eff}(\zeta)\left(E'' - iE'\right)\zeta}{\lambda}\right]d\zeta; \quad (13)$$

$$g(\zeta) = (g_{11} - g_{22})\frac{R_{10}R_{20}}{I_{R0}} + g_{12}\frac{R_{20}^2}{I_{R0}}\exp(i\Delta k\zeta) - g_{12}^*\frac{R_{10}^2}{I_{R0}}\exp(-i\Delta k\zeta); \quad (14)$$

$\boldsymbol{R}_{||}(x) = R_{10}\boldsymbol{e}_1 + R_{20}\boldsymbol{e}_2\exp(i\Delta kx)$ and $\boldsymbol{S}_{||}(x) = S_{10}\boldsymbol{e}_1 + S_{20}\boldsymbol{e}_2 \times \exp(i\Delta kx)$ are the polarisation vectors of the pump and signal waves, respectively, in the absence of the interaction in the crystal; and $I_{R0} = |R_{10}|^2 + |R_{20}|^2 \approx I_0$. The vector $\boldsymbol{R}_{\perp}(x) = R_{20}^*\boldsymbol{e}_1 - R_{10}^*\boldsymbol{e}_2\exp(i\Delta kx)$ characterises the component of the signal-wave light field orthogonal to the polarisation state of the pump field $\boldsymbol{R}_{||}(x)$ ($\boldsymbol{R}_{||}(x)\boldsymbol{R}_{\perp}^*(x) = 0$).

Expressions (12)–(14) describe the polarisation structure $\boldsymbol{S}(x)$ of a weak light wave interacting with a strong pump wave on the photorefractive grating produced in the cubic gyrotropic crystal in an external electric field, which contains both the local ($\sim E'$) and nonlocal ($\sim E''$) components. They are valid in the general case of an arbitrary polarisation of light waves incident on the input face of an arbitrarily oriented sample and impose no restrictions on the direction of the external field if it is applied perpendicular to the x axis ($\boldsymbol{E}_0 || \boldsymbol{K}$).

Note that the appearance of the component with the polarisation vector $\boldsymbol{R}_\perp(x)$ in the polarisation structure $\boldsymbol{S}(x)$ is caused not only by intermode processes with the phase-matching conditions $\boldsymbol{k}_{S1} = \boldsymbol{k}_{R2} - \boldsymbol{K} + \Delta\boldsymbol{k}$ and $\boldsymbol{k}_{S2} = \boldsymbol{k}_{R1} - \boldsymbol{K} - \Delta\boldsymbol{k}$ (see Fig. 1) proceeding with the transformation of the polarisation-state type ($\boldsymbol{e}_2 \to \boldsymbol{e}_1$ and $\boldsymbol{e}_1 \to \boldsymbol{e}_2$) but also by intramode processes ($\boldsymbol{k}_{S1} = \boldsymbol{k}_{R1} - \boldsymbol{K}$ and $\boldsymbol{k}_{S2} = \boldsymbol{k}_{R2} - \boldsymbol{K}$), which proceed without a change in the polarisation state. The intramode processes affect the polarisation component $\sim\boldsymbol{R}_\perp(x)$ of a weak light field due to their different efficiency, which is determined by their tensor convolutions g_{11} and g_{22} (see Table 1). This part of the polarisation component with the vector $\boldsymbol{R}_\perp(x)$ is described by the term proportional to the difference $g_{11} - g_{22}$ in expression (14).

When the light waves incident on the crystal have the same polarisation, the polarisation state of the signal wave $\boldsymbol{S}_{||}(x)$ coincides, in the absence of interaction, with the polarisation state of the pump wave $\boldsymbol{R}_{||}(x)$. When $m(x) \ll 1$, we can assume that $m_0 \approx 2(I_{S0}/I_{R0})^{1/2}$ and the relations $\boldsymbol{R}_{||}(x) = 2\boldsymbol{S}_{||}(x)/m_0$ and $\boldsymbol{R}_\perp(x) = 2\boldsymbol{S}_\perp(x)/m_0$ are valid. If the local component of the spatial-charge field can be neglected ($E' = 0$), then the structure of expression (12) becomes similar to the structure of relations obtained in papers [10, 14, 17].

When the beams incident on the crystal have the same polarisation, the two-wave gain $\Gamma = \ln(I_S/I_{S0})$ of a weak signal wave intensity I_S ($I_{S0} = |S_{10}|^2 + |S_{20}|^2$) can be represented as a sum of two components

$$\Gamma(x) = \Gamma_{||}(x) + \Gamma_\perp(x), \tag{15}$$

where

$$\Gamma_{||}(x) = \frac{2\pi n^3 r_{\text{eff}}(x) E''}{\lambda}, \tag{16}$$

$$\Gamma_\perp(x) = \frac{1}{x}\ln\left\{1 + \left|\frac{\pi n^3 r_{41}\left(E' + \mathrm{i}E''\right)}{\lambda} X(x) \times \exp\left[-\frac{\pi n^3 r_{\text{eff}}(x) E''}{\lambda} x\right]\right|^2\right\}. \tag{17}$$

The first term in (15) is the contribution of the component with the polarisation vector $\boldsymbol{S}_{||}(x)$ to the weak light field intensity. It describes a usual unidirectional energy exchange, which can either enhance a weak light wave (when $\Gamma_{||}(x)$ is positive) or weaken the wave (when $\Gamma_{||}(x)$ is negative). The coefficient $\Gamma_{||}(x)$ is determined only by the nonlocal component E'' of the spatial charge field. A special feature of the unidirectional energy transfer is a change in its direction [a change in the sign of $\Gamma_{||}(x)$] upon the rotation of a sample (Fig. 1) around the x axis through 180°. The modulus of $|\Gamma_{||}(x)|$ does not change in this case.

The second term in (15) is the contribution of the component with the polarisation vector $\boldsymbol{S}_\perp(x)$ orthogonal to $\boldsymbol{S}_{||}(x)$ to the weak light field intensity. This contribution is nonunidirectional because $\Gamma_\perp(x) > 0$ always. The coefficient $\Gamma_\perp(x)$ is determined both by the local (E') and nonlocal (E'') components of the spatial charge field. Due to the nonunidirectional energy exchange, a weak signal wave can be efficiently amplified even in the case of a purely local photorefractive response of the crystal, when $E'' = 0$. The component $\Gamma_\perp$, unlike $\Gamma_{||}$, depends both on the product of the effective electrooptical coefficient by the sample thickness $r_{\text{eff}}(d)d$ ($x = d$) and on the product $r_{\text{eff}}(\xi)\xi$ in the interval $0 \leqslant \xi \leqslant d$, which determines the integral $X(d)$ [see expression (13)]. The exponents of the exponential factors in expression (17), which are proportional to the above products, have real parts with opposite signs. The exponential in the integrand of the integral $X(d)$ (13) is multiplied by the periodic function $g(\xi)$ (14). Therefore, when the sample is rotated through 180° around the x axis, resulting in the change of the signs of the effective electrooptical coefficient $r_{\text{eff}}(\xi)$ and of the function $g(\xi)$, the component $\Gamma_\perp(d)$ changes.

Fig. 2 shows the dependences of the total gain Γ (curves *1*) and its components $\Gamma_{||}$ (curves *2*) and $\Gamma_\perp$ (curves *3*) on the sample thickness d for the longitudinal geometry of the interaction in a $Bi_{12}TiO_{20}$ crystal with typical parameters $n = 2.58$, $\rho = 6$ deg mm^{-1}, and $r_{41} = -5$ pm V^{-1} at a wavelength of 633 nm. We assumed in calculations that the light waves at the boundary $x = 0$ were linearly polarised perpendicular to the plane of incidence, and the electric field strength E_0 was positive and equal to 10 kV cm^{-1}. The solid curves in Fig. 2 correspond to the sample orientation at which the positive direction of the z axis in the coordinate system chosen by us (Fig. 1) coincides with the crystallographic axis [001]. The dashed curves correspond to the sample orientation that is obtained from the previous

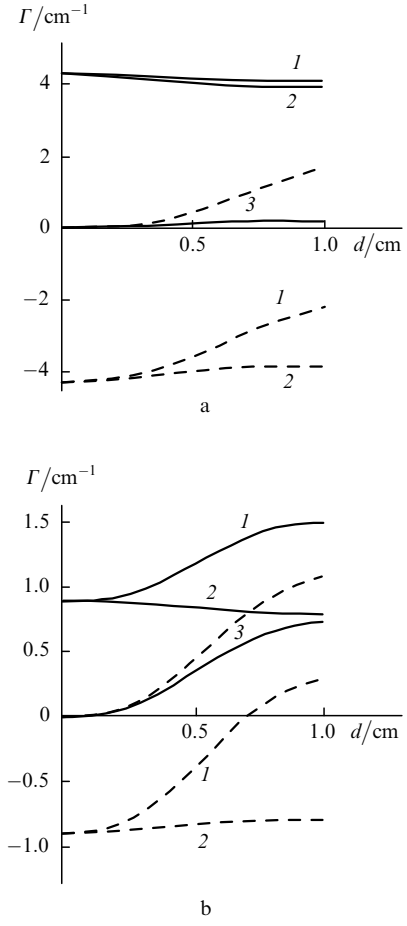

Figure 2. Dependences of the two-wave gain (*1*) and its unidirectional (*2*) and nonunidirectional (*3*) components on the thickness of the $Bi_{12}TiO_{20}$ crystal for the longitudinal geometry of the interaction at the acceptor concentrations $N_a = 10^{21}$ (a) and 10^{22} m^{-3} (b).

orientation by rotating the sample through 180° around the x axis. In this case, the z axis is directed along the $[00\bar{1}]$ axis of the crystal.

The curves in Fig. 2a were calculated for the sample with the acceptor concentration $N_a = 10^{21}$ m^{-3} and the grating period $\Lambda = 17$ μm at which the nonlocal component of the spatial-charge field is maximum ($E'' = 5$ kV cm^{-1}) and the usual (unidirectional) energy exchange is highly efficient ($\Gamma_{\|} \approx 4.3$ cm^{-1}) and only weakly depends on d (see curves *2*). This is explained by the fact that in the case of longitudinal geometry of the interaction ($\boldsymbol{K} \| [001]$), the effective electrooptical coefficient

$$r_{\text{eff}}^{[001]}(x) = -\frac{r_{41}}{2}\left\{1 + \frac{1}{1+(\beta/2)^2} \times \left[\left(\frac{\beta}{2}\right)^2 + \frac{\sin\left[2\rho x\left[1+(\beta/2)^2\right]^{1/2}\right]}{2\rho x\left[1+(\beta/2)^2\right]^{1/2}}\right]\right\}, \quad (18)$$

[where $\beta = \pi n^3 r_{41} E_0/(\rho\lambda)$] is mainly determined by the intramode process. This process is described by the term $[1+2(\beta/2)^2]/[1+(\beta/2)^2]$, which does not depend on the coordinate x and is close to 2 in a strong external field ($E_0 \sim 10$ kV cm^{-1}). The contribution of the intermode process is determined by the term $\sin\{2\rho x[1+(\beta/2)^2]^{1/2}\}/\{2\rho x[1+(\beta/2)^2]^{3/2}\}$, which does not exceed 0.16. Therefore, the deviation of the polarisation state of the interacting waves from the optimal state caused by the optical activity and induced linear birefringence results in a small decrease in $r_{\text{eff}}^{[001]}$ and $\Gamma_{\|}$ with increasing sample thickness.

In the case of the longitudinal geometry of the interaction, the dependence of the product $r_{\text{eff}}^{[001]}(x)x$ on the coordinate is determined by the linear function. The coefficient $\Gamma_{\perp}^{+}$, corresponding to the sample orientation at which the z axis coincides with the crystallographic axis [001] and the coefficient $r_{\text{eff}}(x)$ is positive (solid curve *3* in Fig. 2a), is smaller than the coefficient $\Gamma_{\perp}^{-}$ corresponding to another orientation at which the z axis coincides with the crystallographic axis $[00\bar{1}]$ and the coefficient $r_{\text{eff}}(x)$ is negative (dashed curve *3* in Fig. 2a). When the condition $|2\pi n^3 r_{\text{eff}}(x)E''x/\lambda| \ll 1$ is fulfilled, the nonunidirectional component $\Gamma_{\perp}$ of the total gain increases proportionally to x^2.

The coefficient $\Gamma_{\perp}^{+}$ reaches the maximum value $\Gamma_{\perp\,\max}^{+} = 0.17$ cm^{-1} at $x \approx 0.78$ cm and then decreases to zero at $x \to \infty$. For this reason, the total gain $\Gamma(x)$ for the first orientation only slightly differs from its positive unidirectional component. In the case of the second orientation, the coefficient $\Gamma_{\perp}^{-}$ monotonically increases with x and reaches the maximum value $\Gamma_{\perp\,\max}^{-} \approx 3.57$ cm^{-1} for $x \sim 10$ cm. Therefore, upon the interaction in thick samples oriented so that the positive direction of the z axis coincides with the crystallographic axis $[00\bar{1}]$, the positive nonunidirectional component is comparable with the negative unidirectional component, while the modulus of the total gain $\Gamma(x)$ is small, for example, $\Gamma(0.1) \approx 0.33$ cm^{-1}.

The curves in Fig. 2a correspond to the local-component strength $E' = 5.2$ kV cm^{-1}, which is lower than the maximum value $E'_{\max} = E_0$, which is reached at high strengths of the trap saturation field $E_q \gg E_0$ [see expression (3)]. The curves in Fig. 2b were calculated for the sample with the acceptor concentration $N_a = 10^{22}$ m^{-3}. In this case, $E' = 9.9$ kV cm^{-1}, which is virtually equal to E_0, while the strength of the nonlocal component $E'' = 1$ kV cm^{-1} is smaller approximately by a factor of five than the strength corresponding to the case considered above. This results in a decrease in the unidirectional component $\Gamma_{\|}$ of the total gain Γ and in an increase in the relative contribution of the nonunidirectional component $\Gamma_{\perp}$, leading to a strong dependence of the gain Γ on the sample thickness already for $d \geqslant 2$ mm. For $d \geqslant 7.5$ mm, the component $\Gamma_{\perp}^{-}$ becomes greater than $|\Gamma_{\|}|$, and a weak light wave is amplified for both orientations of the sample. In this case, unlike the previous one, the maximum positive total gain $\Gamma \approx 1.9$ cm^{-1} is reached in a thick sample with $d \approx 0.92$ cm rather than in a thin sample.

Fig. 3 shows the dependences of quantities Γ, $\Gamma_{\|}$ and $\Gamma_{\perp}$ on the sample thickness d calculated for the transverse geometry of the interaction. The solid curves in Fig. 3 correspond to the sample orientation at which the positive direction of the z axis coincides with the crystallographic axis $[\bar{1}10]$, while the dashed curves correspond to the sample orientation at which the z axis is directed along the $[\bar{1}10]$ axis of the crystal. For this geometry and the polarisation of light waves at the boundary $x = 0$ being linear and orthogonal to the plane of incidence, a photorefractive grating is produced only due to intermode processes, and the expression

$$r_{\text{eff}}^{[\bar{1}10]}(x) = r_{41}\frac{\sin^2\left[\rho x\left(1+\beta^2\right)^{1/2}\right]}{\rho x\left(1+\beta^2\right)} \quad (19)$$

for the effective electrooptical coefficient does not contain the term independent of x.

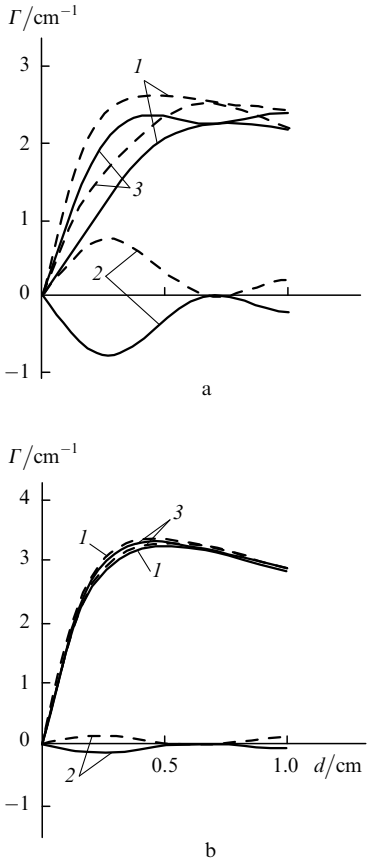

Figure 3. Dependences of the two-wave gain (*1*) and its unidirectional (*2*) and nonunidirectional (*3*) components on the thickness of the $Bi_{12}TiO_{20}$ crystal for the transverse geometry of the interaction at the acceptor concentrations $N_a = 10^{21}$ (a) and 10^{22} m^{-3} (b).

As the sample thickness is increased, the value of $r_{\rm eff}^{[\bar{1}10]}$ decreases nonmonotonically, so that the contribution of the unidirectional component $\Gamma_{||}$ to the total gain is small compared to that from the nonunidirectional component $\Gamma_{\perp}$. A comparison of Figs 3a and 3b shows that in the case of transverse geometry, unlike the longitudinal one (see Fig. 2), the increase in the local component E' of the field amplitude of the spatial charge enhances the total two-wave gain $\Gamma(d)$. The coefficient $\Gamma_{\perp}^{+}$ in the case of the positive effective electrooptical coefficient $r_{\rm eff}(x)$ (dashed curve *3*) can be either larger or smaller than the coefficient $\Gamma_{\perp}^{-}$ for the negative $r_{\rm eff}(x)$ (solid curve *3*).

4. Effect of an external electric field on the efficiency of energy transfer for transverse geometry

The characteristic feature of the transverse geometry of interaction in strong electric fields $E_0 \sim 10$ kV cm^{-1} is the amplification of a weak signal wave for both orientations of a sample, which can be obtained from each other by rotating the sample around the vertical axis (Fig. 3). However, when E_0 is decreased, such nonunidirectional energy transfer is violated. The numerical analysis shows that for the parameters of the $Bi_{12}TiO_{20}$ crystal presented above and the spatial period $\Lambda = 17$ μm of the photorefractive grating used in calculations, the nonunidirectional energy transfer can occur for all x if the external field does not exceed the value $E_{\rm min} = 1.73$ kV cm^{-1}.

Fig. 4 shows the dependences of the total two-wave gain Γ and of its unidirectional ($\Gamma_{||}$) and nonunidirectional ($\Gamma_{\perp}$) components on the external field strength E_0 for the case when the positive direction of the z axis coincides with the crystallographic axis $[\bar{1}10]$, $d = 1$ cm, and the acceptor concentration $N_{\rm a} = 10^{21}$ m^{-3}. When polarisation of the pump wave at the boundary $x = 0$ is linear and orthogonal to the plane of incidence, the effective electrooptical coefficient (19) is a symmetric function of E_0 ($r_{\rm eff}(E_0) = r_{\rm eff}(-E_0)$), while the integral (13) is an antisymmetric function of E_0 ($X(E_0) = -X(-E_0)$). In this case [see expressions (16) and (17)], both components of the gain Γ are symmetric functions of E_0, as demonstrated in Fig. 4a. One can see that the component $\Gamma_{\perp}$ for small external fields $|E_0| <$ 1.73 kV cm^{-1} is less than the modulus of the component $\Gamma_{||}$, which is negative. In this region of values of E_0, the signal wave is weakened due to the interaction with the reference wave. If the positive direction of the z axis coincides with the crystallographic axis $[1\bar{1}0]$, then the signal wave is amplified both due to unidirectional and nonunidirectional energy exchange. For this orientation of the sample, $\Gamma > 0$ for all E_0.

For the right (rig) or left (lef) circular polarisation of the waves incident on the crystal, the effective electrooptical coefficient can be written in the form

$$r_{\rm eff\,rig,\,eff\,lef}^{[110]}(x) = \pm r_{41}\,\frac{\beta}{1+\beta^2}\left\{1 - \frac{\sin[2\rho x(1+\beta^2)^{1/2}]}{2\rho x(1+\beta^2)^{1/2}}\right\}, \quad (20)$$

from which it follows that it is an antisymmetric function of the external field ($\beta_0 \sim E_0$). The dependences of the two-wave gain Γ and of its nonunidirectional component on E_0 in Fig. 4b contain both symmetric and antisymmetric components. In the region of positive E_0, the gain $\Gamma_{\perp}$ is greater than the modulus of the gain $\Gamma_{||}$, which is negative

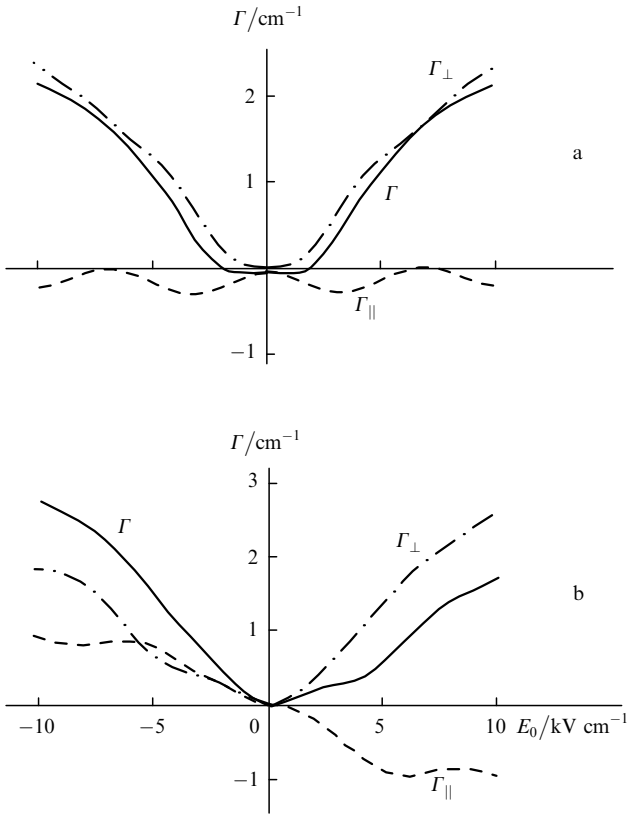

Figure 4. Dependences of the two-wave gain Γ and its unidirectional ($\Gamma_{||}$) and nonunidirectional ($\Gamma_{\perp}$) components on the external electric field strength for the transverse geometry of the interaction in a 1-cm thick $Bi_{12}TiO_{20}$ crystal in the case of (a) linear and (b) circular polarisation.

here, and any light wave is amplified for any E_0. The energy transfer efficiency is higher for the negative external field E_0 and lower for positive field than in the case of linear polarisation of the incident waves (cf. Fig. 4a). In the case of circular polarisation of the incident waves, the energy transfer remains nonunidirectional for any thickness d of the sample and any E_0. In this case, the rotation of the sample around the [110] axis through 180° does not change the two-wave gain.

5. Energy exchange for an arbitrary modulation coefficient

The use of the general expressions derived above for analysis of the polarisation structure and intensity of a weak signal wave upon its interaction with a reference wave on the photorefractive grating in a cubic gyrotropic crystal in an external electric field is limited by the fixed pump-wave light field approximation. This approximation is valid for a small modulation coefficient $m(x) \ll 1$ of the interference pattern. Because the complete system of coupled-wave equations (5)–(8) was obtained by neglecting nonlinear [in $m(x)$] corrections to the amplitude of the spatial-charge field, its numerical integration cannot completely describe the interaction for large modulation coefficients. However, the extrapolation of the solutions of these equations to the case $m(x) \sim 1$ allows us to observe the type of variations occurring during the levelling of intensities of the interacting light waves.

Fig. 5 shows the dependences of the two-wave gain on the interaction length for different modulation coefficients m_0 at the boundary $x = 0$, which were calculated by the known formula [4, 8, 9]

$$\Gamma_{\rm sd} = \frac{1}{x}\ln\left[\frac{|S_1^{\rm sd}(x)|^2 + |S_2^{\rm sd}(x)|^2}{|S_{10}|^2 + |S_{20}|^2} \times \frac{|R_{10}|^2 + |R_{20}|^2}{|R_1^{\rm sd}(x)|^2 + |R_2^{\rm sd}(x)|^2}\right], \quad (21)$$

where the superscript sd means that the scalar amplitudes of the natural waves are the solution of the self-consistent self-diffraction problem (3), (5)–(8) and satisfy to the law of conservation of energy (9). The calculations were performed for the transverse geometry at the acceptor concentration $N_a = 10^{21}$ m^{-3} and the parameters of the $Bi_{12}TiO_{20}$ crystal presented above. The solid curves in Fig. 5, as in Fig. 3, correspond to the sample orientation at which the positive direction of the z axis coincides with the crystallographic axis $[\bar{1}10]$, while the dashed curves correspond to the sample orientation at which the z axis is directed along the $[1\bar{1}0]$ axis of the crystal.

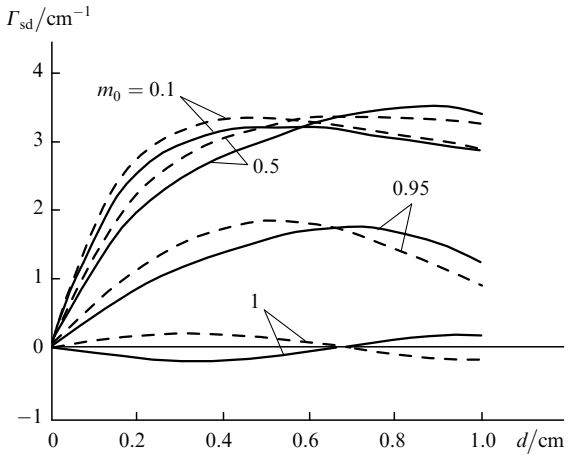

Figure 5. Dependences of the two-wave gain on the thickness of the $Bi_{12}TiO_{20}$ crystal for different modulation coefficients m_0 of the interference grating on the input face in the case of linear polarisation of the incident wave.

One can see from Fig. 5 that the nonunidirectional energy exchange is observed for all $m_0 < 1$, and the dependences of the two-wave gain $\Gamma_{\rm sd}$ calculated for opposite directions of the z axis are symmetric with respect to the abscissa only for $m_0 = 1$. This corresponds to the disappearance of the nonunidirectional energy transfer at the equal intensities of the incident waves.

Note that the gain $\Gamma_{\rm sd}$ depends on m_0 nonmonotonically for samples of thickness $d > 0.55$ cm. The numerical calculation showed that this dependence is caused by the contribution of the local component E' of the spatial charge field to the energy exchange. The nonmonotonic dependence of the two-wave gain on the ratio of the intensities of light beams at the input face of the sample is not typical for most of experimental and theoretical studies of the two-wave interaction in photorefractive crystals [8, 9, 22, 23]. The exception is the experiments on the two-wave interaction in a $Bi_{12}SiO_{20}$ crystal in an external meander field performed recently [24]. However, the presence of the point of inflexion in the dependence $\Gamma(m_0)$ is attributed in this paper to the influence of the corrections to the first-harmonic amplitude of the spatial-charge field, which are nonlinear over the modulation coefficient.

6. Conclusions

Our analysis of the steady-state symmetric two-wave interaction in a cubic gyrotropic crystal has shown the possibility of efficient energy exchange on the unshifted component of a transmission photorefractive grating. The contribution of such energy exchange to the intensity of a weak light wave is always positive and it is caused by the appearance in its polarisation structure of the component whose polarisation is orthogonal to that of a strong pump wave. In a particular case of the interaction in the $Bi_{12}TiO_{20}$ crystal, when the grating vector is oriented along the $[\bar{1}10]$ axis and light waves propagating in the plane (001) are polarised perpendicular to this plane or have circular polarisation, the coefficient of nonunidirectional energy transfer can exceed that of the unidirectional energy transfer for any sample thickness if the external field exceeds the threshold field, which is determined by the photorefractive parameters of the sample and by the spatial period of the grating. For the light waves having the same intensity at the crystal boundary, the contribution from the nonunidirectional energy exchange to the two-wave gain is zero.

References

1. Chen F S *Appl. Phys.* **40** 3389 (1969)
2. Vahey D W *Appl. Phys.* **46** 3510 (1975)
3. Kukhtaraev N V, Markov V B, Odulov S G *Opt. Commun.* **23** 338 (1977)
4. Sturman B I *Zh. Tekh. Fiz.* **48** 1010 (1978)
5. Kukhtaraev N V, Markov V B, Odulov S G, Soskin M S, Vinetskii V L *Ferroelectrics* **22** 949 (1979)
6. Kukhtarev N V, Markov V B, Odulov S G *Zh. Tekh. Fiz.* **50** 1905 (1980)
7. Solymar L, Heaton J M *Opt. Commun.* **51** 338 (1984)
8. *Photorefractive Materials and Their Applications*, Eds. Gunter P, Huignard J P (Berlin: Springer-Verlag, 1988, vol. 1; 1989, vol. 2)
9. Petrov M P, Stepanov S I, Khomenko A V *Fotorefraktivnye kristally v kogerentnoi optike* (Photorefractive Crystals in Coherent Optics) (St. Petersburg: Nauka, 1992)
10. Litvinov R V, Shandarov S M *Opt. Spektrosk.* **83** 334 (1997)
11. Shamonina E, Kemenov V P, Ringhofer K H, Cedilink G, Kiessling A, Kowarschic R *J. Opt. Soc. Am. B: Opt. Phys.* **15** 2552 (1998)
12. Shepelevich V V, Hu Y, Shamonina E, Ringhofer K H *Appl. Phys. B* **68** 923 (1999)
13. Hu Y, Ringhofer K H, Sturman B I *Appl. Phys. B* **68** 931 (1999)
14. Krasnoperov V Yu, Litvinov R V, Shandarov S M *Fiz. Tverd. Tela* **41** 632 (1999)
15. Sturman B I, Podivilov E V, Ringhofer K H, Shamonina E, Kemenov V P, Nippolainen E, Prokofiev V V, Kamshilin A A *Phys. Rev. E* **60** 3332 (1999)
16. Shepelevich V V, Firsov A A *Kvantovaya Elektron.* **30** 60 (2000) [*Quantum Electron.* **30** 60 (2000)]
17. Litvinov R V, Shandarov S M, Chistyakov S G *Fiz. Tverd. Tela* **42** 1397 (2000)
18. Odulov S G, Soskin M S, Khizhnyak A I *Lazery na dinamicheskikh reshetkakh* (Dynamic Grating Lasers) (Moscow: Nauka, 1990)
19. Yeh P *Proc. IEEE* **80** 436 (1992)

20. Litvinov R V, Polkovnikov S I, Shandarov S M *Kvantovaya Elektron*. **31** 167 (2001) [*Quantum Electron*. **31** 167 (2001)]
21. Sirotin Yu I, Shaskol'skaya M P *Osnovy kristallofiziki* (Fundamentals of Crystal Physics) (Moscow: Nauka, 1975)
22. Millerd J E, Garmire E M, Klein M B, Wecher B A Stohkendl F P, Brost G A *J. Opt. Soc. Am. B: Opt. Phys.* **9** 1449 (1992)
23. Kobozev O V, Madel' A E, Shandarov S M, Petrov S A, Kargin Yu F *Kvantovaya Elektron.* **30** 514 (2000) [*Quantum Electron*. **30** 514 (2000)]
24. Shandarov S M, Krasnoperov V Yu, Kartashev V A, Veretennikov S Yu, Mandel' A E, Kargin Yu F, Litvinov R V, Pitchenko S N *Neorg. Mater.* **37** 728 (2001)